

Mitochondria Targeted and Intracellular Biothiol Triggered Hy-perpolarized ^{129}Xe Magneto-Fluorescent Biosensor

Qingbin Zeng^{a, b‡}, Qianni Guo^{a, b‡}, Yaping Yuan^{a, b}, Yuqi Yang^a, Bin Zhang^a, Lili Ren^a, Xiaoxiao Zhang^a, Qing Luo^{a, b}, Maili Liu^{a, b}, Louis-S. Bouchard^c, Xin Zhou^{a, b*}

^a Key Laboratory of Magnetic Resonance in Biological Systems, State Key Laboratory of Magnetic Resonance and Atomic and Molecular Physics, National Center for Magnetic Resonance in Wuhan, Collaborative Innovation Center of Chemistry for Life Sciences, Wuhan Institute of Physics and Mathematics, Chinese Academy of Sciences, Wuhan 430071, P. R. China.

^bUniversity of Chinese Academy of Sciences, Beijing 100049, P. R. China.

^c Departments of Chemistry & Biochemistry and of Bioengineering, California Nano Systems Institute, Jonsson Comprehensive Cancer Center, The Molecular Biology Institute, University of California, Los Angeles CA 90095, USA.

[‡]These authors contributed equally.

* E-mail: xinzhou@wipm.ac.cn

Supporting Information

Contents

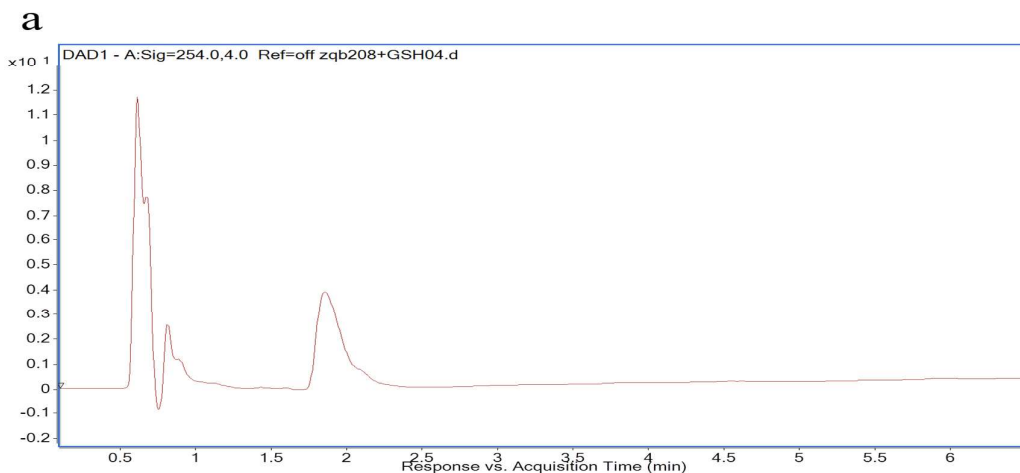
1. Materials and Instruments.
2. LC-MS Spectroscopic Analysis
3. Proposed mechanism of biosensor 7 reaction with biothiols
4. Additional Fluorescence Spectra
5. Additional ^{129}Xe NMR and Hyper-CEST NMR Spectra
6. Detection limit of biosensor 7
7. Additional Cellular Fluorescence Imaging
8. Additional Cellular Hyper-CEST Spectra
9. ^1H -NMR, ^{13}C -NMR and ESI-HRMS Spectra

1. Materials and Instruments.

Unless otherwise stated, all reagents were purchased from commercial suppliers and were used without further purification. Triphenylphosphonium, 3-Bromopropylamine hydrobromide, 4-Bromonaphthalic anhydride, 3-Aminopropanoic acid, 4-Dimethylaminopyridine (DMAP), 2, 2'-Dithiodiethanol, 1-Butanol, Methyl t-butyl ether, Ethyl 2-bromoacetate, NaN_3 , NaHCO_3 , K_2CO_3 , NaOH , Na_2CO_3 , Na_2HPO_4 , NaH_2PO_4 , HCl , Dimethylformamide (DMF), Acetone, Methanol, Ethanol, Tetrahydrofuran (THF), Dichloromethane (DCM) were purchased from Sinopharm Chemical Reagent Co. Ltd.; Cryptophanol-A was purchased from Wuhan Liperen Sci-Tech Co., Ltd. 1-(3-Dimethylaminopropyl)-3-ethylcarbodiimide hydrochloride (EDCI) was purchased from Shanghai Medpep Co. Ltd.; 1-Hydroxybenzotriazole (HOBT) was purchased from GL Biochem Ltd.; N-ethylmaleimide, Cremophor[®] EL, N,N-Diisopropylethylamine (DIPEA) were purchased from Aladdin Chemistry Co. Ltd.; Mitro-Tracker Red was purchased from Invitrogen Co. Ltd.; Lyso-Tracker red and ER-Tracker red were purchased from Beyotime Biotechnology Co. Ltd., all reagents were of analytical grade. Dimethyl sulfoxide (DMSO) was purchased from Tianjin Kemiou Chemical Reagent Co. Ltd., this reagent was of spectral grade.

^1H NMR and ^{13}C NMR spectra were recorded on Bruker AVANCE 500 spectrometer, using TMS as internal standard. ^{129}Xe NMR spectra were recorded on a 400 MHz Bruker AV400 wide bore spectrometer. High resolution mass spectra (HRMS) were taken on an Agilent 6530 Accurate-Mass Q-TOF spectrometer. The pH value was acquired by a Mettler Toledo SevenEasy pH meter. UV-Vis spectra were obtained on a Thermo Scientific evolution 220 UV-Vis spectrometer. Fluorescence spectra were recorded with an Edinburgh FS5 fluorescence spectrophotometer. Thin layer chromatography (TLC) was performed using silica gel plates with UV light at 254 nm for detection. Confocal images were taken on a Nikon Confocal Laser Scanning Microscope.

2. LC-MS Spectroscopic Analysis



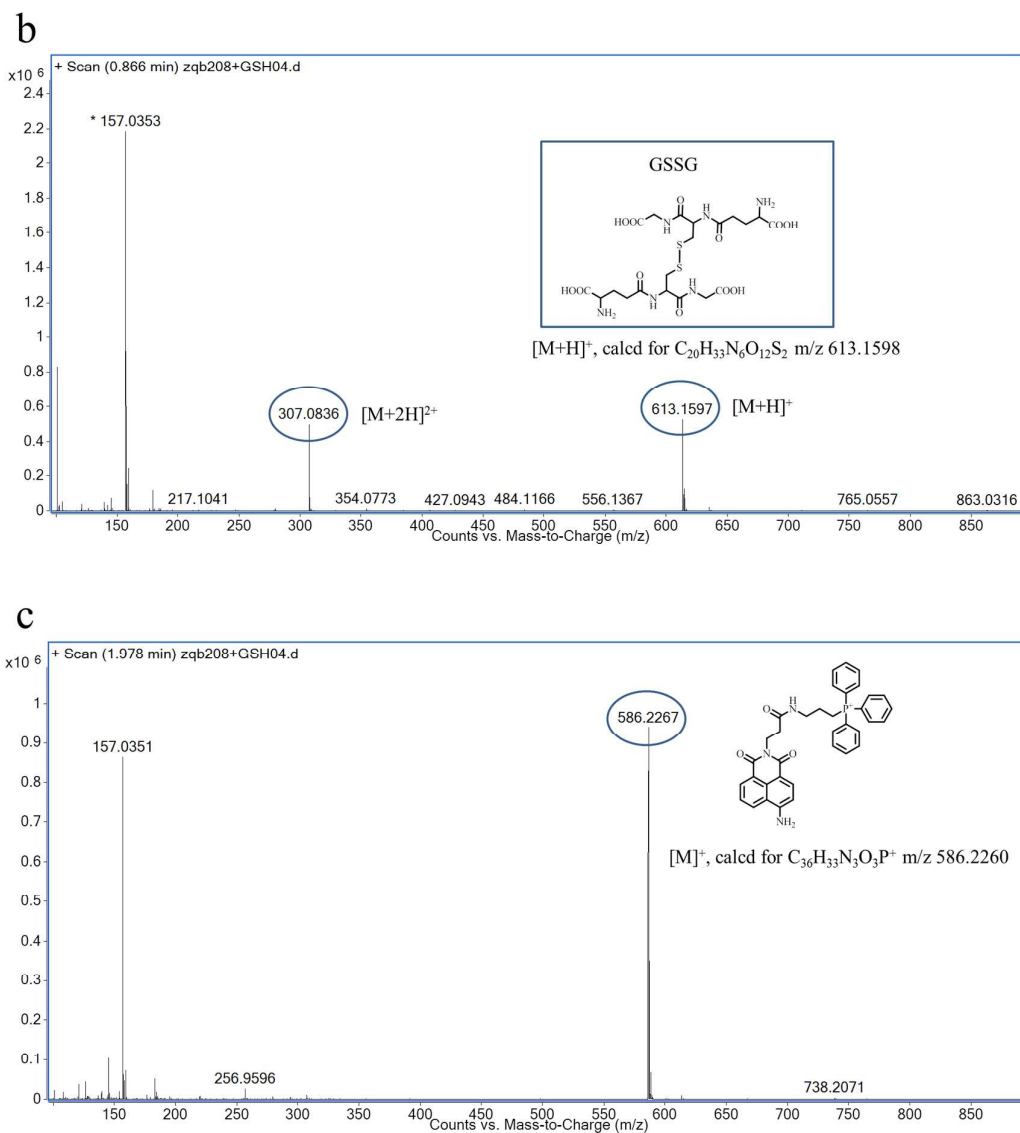
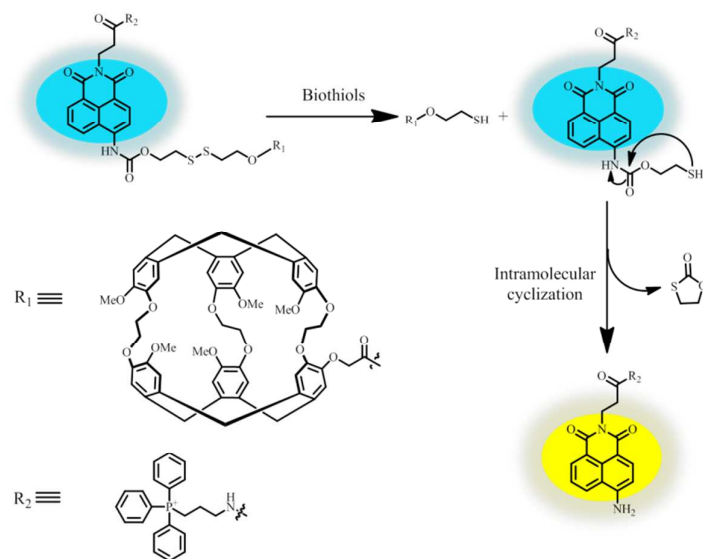


Figure S1. LC-MS analysis of biosensor **7** after reacted with GSH at 37 °C for 2 h. (a) LC analysis of biosensor **7** after reacted with GSH. (b) and (c) MS analysis of biosensor **7** after reacted with GSH.

3. Proposed mechanism of biosensor **7** reaction with biothiols



Scheme S1. Proposed mechanism of biosensor **7** reaction with biothiols.

4. Additional Fluorescence Spectra

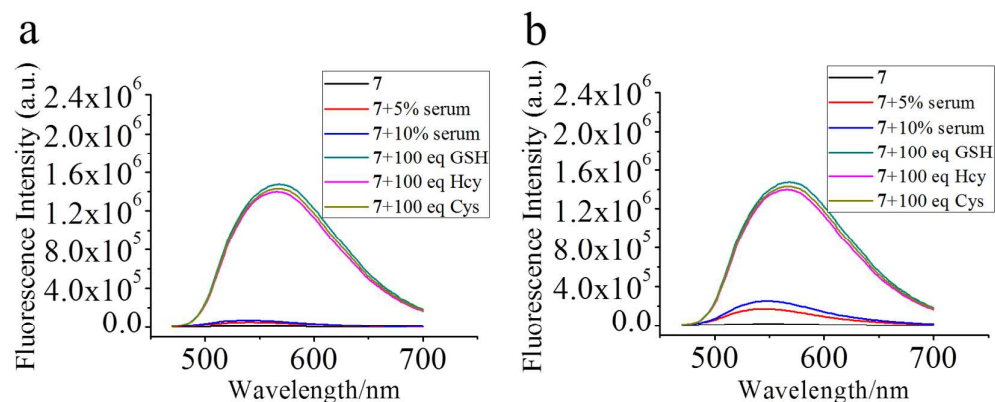


Figure S2. Fluorescence response of biosensor **7** ($5 \mu\text{M}$) for different biothiols and serum. (a) After the biothiols and serum reacted with biosensor **7** for 3 h at room temperature. (b) After the biothiols and serum reacted with the biosensor **7** for 30 min at 37°C . All spectra were acquired at room temperature in PBS buffer ($\text{pH}=7.4$, 20 mM), containing $20\% \text{ DMSO (v/v)}$.

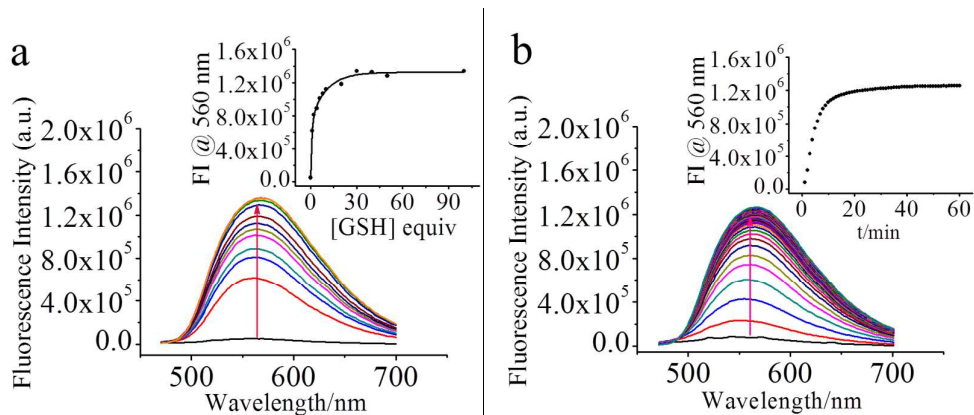


Figure S3. (a) Fluorescence response of biosensor **7** ($5\ \mu\text{M}$) for different concentrations of GSH. Inset: Change in fluorescence intensity at 560 nm as a function of GSH concentration. All spectra were acquired at room temperature after incubation at $37\ ^\circ\text{C}$ for 2 h in PBS buffer (pH=7.4, 20 mM), containing 20% DMSO (v/v). (b) Time-dependent fluorescence spectra of biosensor **7** ($5\ \mu\text{M}$) treated by GSH ($500\ \mu\text{M}$). Inset: Change in fluorescence intensity at 560 nm as a function of time. All spectra were acquired at $37\ ^\circ\text{C}$ in PBS buffer (pH=7.4, 20 mM) containing 20% DMSO (v/v).

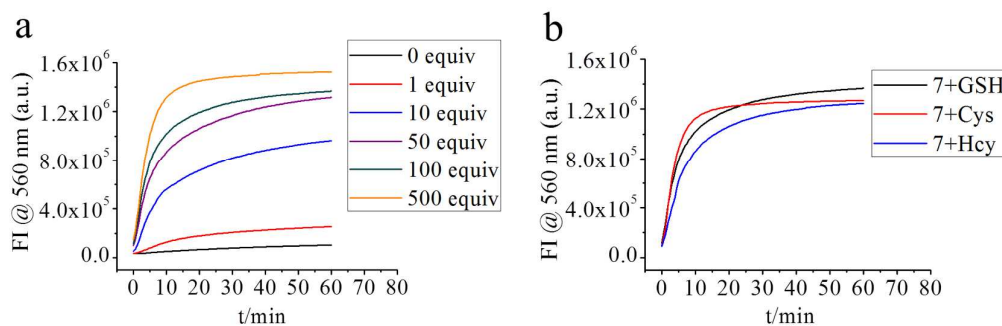


Figure S4. Kinetic scan of biosensor **7** ($5\ \mu\text{M}$) treated by different concentrations of GSH and different biothiols. (a) Fluorescence response of biosensor **7** for different concentrations of GSH. (b) Fluorescence response of biosensor **7** for different analytes. All spectra were acquired at $37\ ^\circ\text{C}$ in PBS buffer (20 mM), containing 20% DMSO (v/v).

5. Additional ^{129}Xe NMR and Hyper-CEST ^{129}Xe NMR Spectra

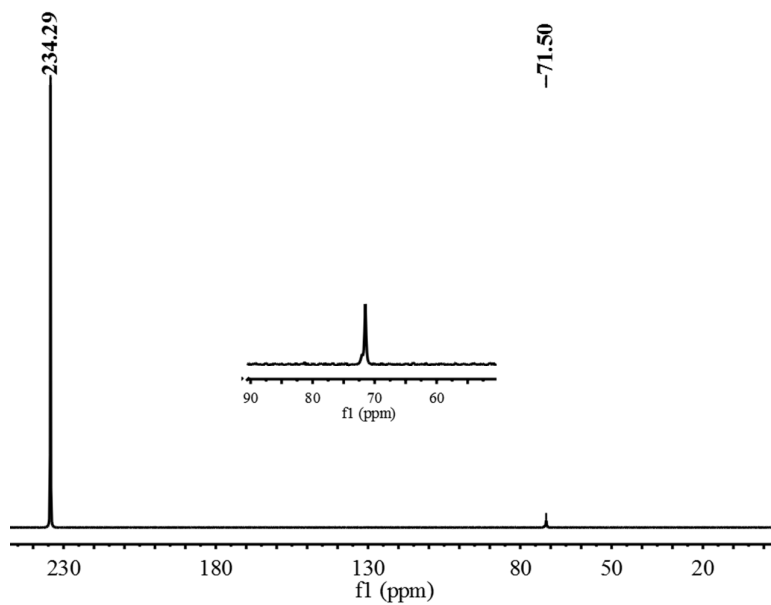


Figure S5. ^{129}Xe NMR spectra of biosensor **7** (25 μM) was acquired at room temperature without heating in PBS buffer (pH=7.4, 20 mM), containing 50% DMSO (v/v). (ns=16, LB=10 Hz).

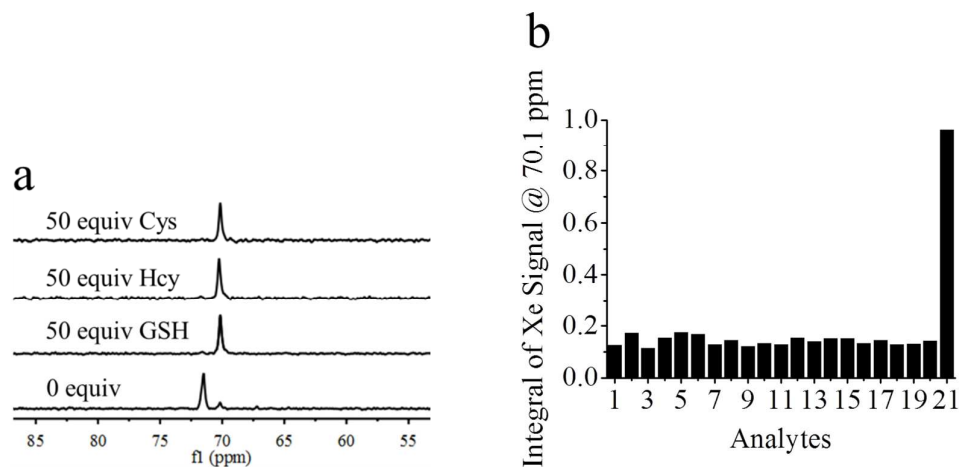


Figure S6. ^{129}Xe NMR spectra (average of 16 scans, line-broadening=10 Hz) of biosensor **7** (25 μM) response to different analytes. (a) ^{129}Xe NMR spectra of biosensor **7** response to biothiols (GSH, Hcy, Cys). (b) Integral of ^{129}Xe NMR signal at 70.1 ppm of biosensor **7** response to nonthiol amino acids (1, only biosensor; 2, Val; 3, Leu; 4, Ile; 5, Phe; 6, Trp; 7, Met; 8, Pro; 9, Gly; 10, Ser; 11, Thr; 12, Tyr; 13, Asn; 14, Gln; 15, His; 16, Lys; 17, Arg; 18, Asp; 19, Glu; 20, Ala; 21, GSH). The concentrations of biothiols, nonthiol amino acids were kept at 1.25 mM. All spectra were acquired at room temperature after heated at 37 $^{\circ}\text{C}$ for 2 h in PBS buffer (pH=7.4, 20 mM), containing 50% DMSO (v/v).

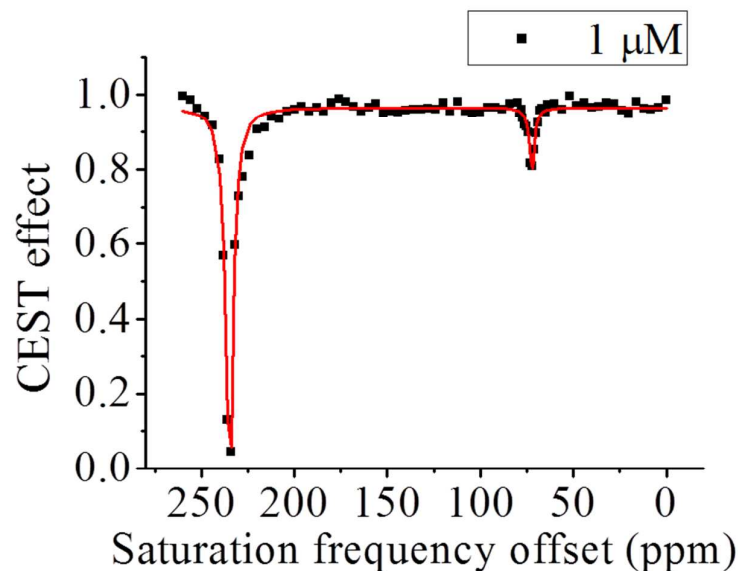


Fig S7. Hyper-CEST spectrum of the biosensor **7** ($1\ \mu\text{M}$) in PBS buffer, (pH=7.4, 20 mM), containing 50% DMSO (v/v). The spectrum was measured with a 10 s saturation pulse with of amplitude $13\ \mu\text{T}$, and the frequency interval from 64 ppm to 80 ppm is 1 ppm, while the frequency interval from 228-240 ppm is 2 ppm, and the frequency interval of the rest spectrum is 4 ppm. Temperature was set to 298 K.

6. Detection limit of biosensor 7

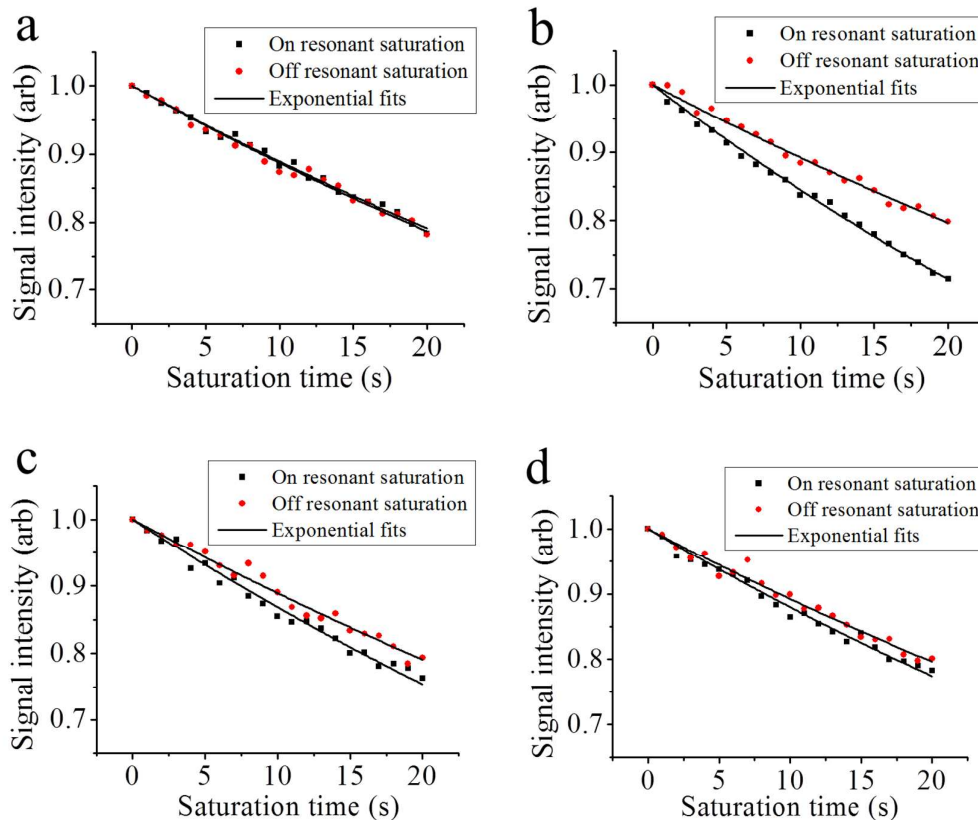


Figure S8. Saturation profiles of different concentration biosensor **7** and 20 mM phosphate buffer. (a) 20 mM phosphate buffer. (b) 50 nM biosensor **7** in PBS buffer, containing 50% DMSO. (c) 500 pM biosensor **7**, containing 50% DMSO. (d) 200 pM biosensor **7**, containing 50% DMSO. All samples were saturated by a cw-saturation pulse with a 13 μ T field. Each saturation profile was fit to an exponential decay equation [$f(t) = \exp(-t/\tau)$].

7. Additional Cellular Fluorescence Imaging

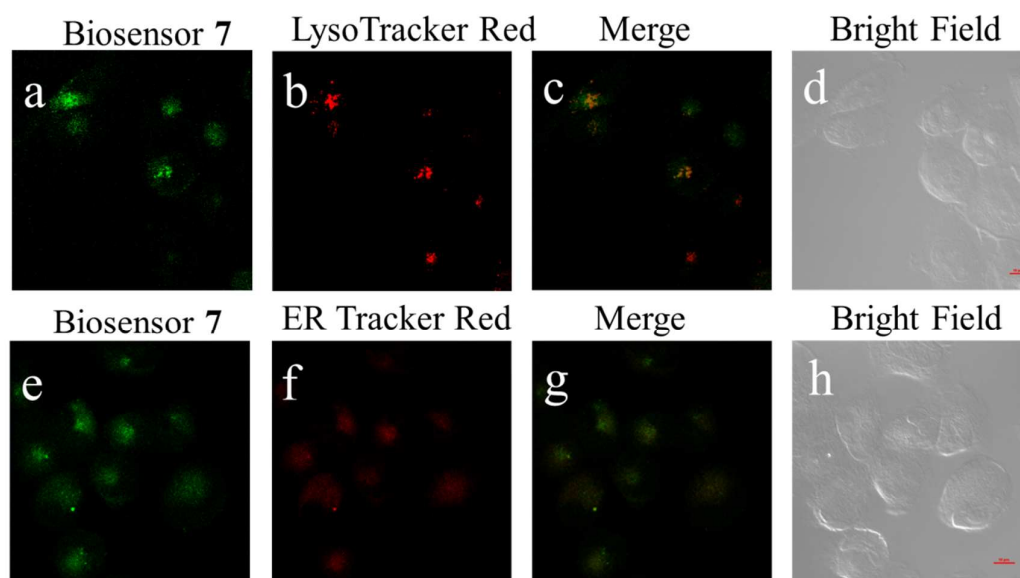


Figure S9. Fluorescence images of H1299 cells treated by biosensor **7** and Lyso-Tracker Red or ER-Tracker Red. After the cells incubated with biosensor **7** (5.0 μ M) at 37 $^{\circ}$ C for 20 min, the medium was replaced by fresh medium containing Lyso-Tracker Red or ER-Tracker Red (0.1 μ M) and incubated for another 20 min. (a, b, c, d) Cells treated by biosensor **7** and Lyso-Tracker Red. (e, f, g, h) Cells treated by biosensor **7** and ER-Tracker Red. Images for biosensor **7** and Lyso-Tracker Red or ER-Tracker Red were obtained after excitation at 488 and 561 nm. Scar bar 10 μ m.

Table S1 The colocalization coefficient of biosensor **7** with MitoTracker Red, Lyso Tracker Red, and ER Tracker Red. The colocalization coefficient analysis via matlab 2011.

	Mito-Tracker Red	Lyso-Tracker Red	ER-Tracker Red
colocalization coefficient	0.72	0.23	0.51

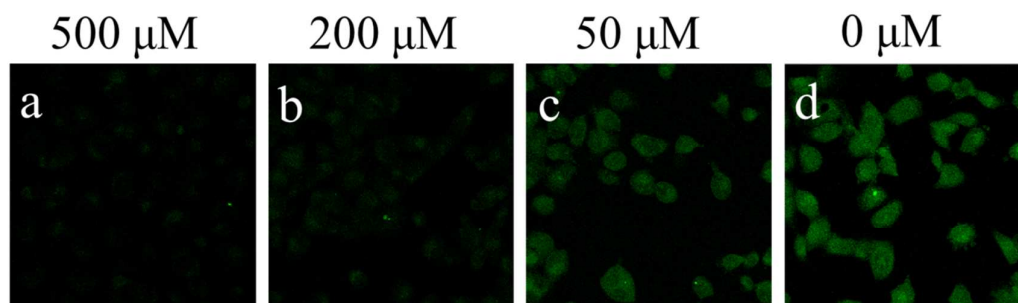


Figure S10. Fluorescence images of H1299 cells treated by biosensor **7** and different concentration of NEM. After the cells incubated with NEM (0 μM , 50 μM , 200 μM , 500 μM) at 37 $^{\circ}\text{C}$ for 30 min, the medium was replaced by fresh medium containing biosensor **7** (5 μM) and incubated for another 30 min at 37 $^{\circ}\text{C}$. Images for biosensor **7** were obtained after excitation at 488 nm.

8. Additional Cellular Hyper-CEST Spectra

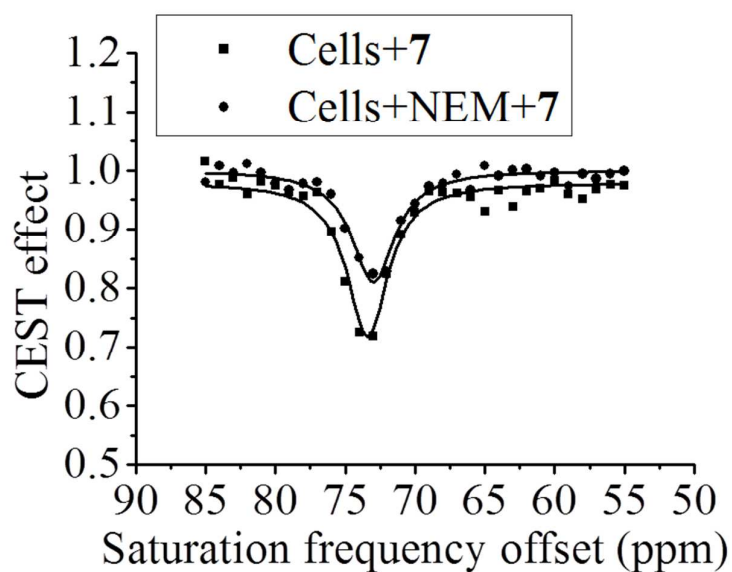


Figure S11. Hyper-CEST spectra for biosensor **7** in lung cancer cells (H1299). (\blacktriangle) After the biosensor **7** incubated with H1299 at 37 $^{\circ}\text{C}$ for 2 h, the hyper-CEST spectrum was acquired. (\blacksquare) After the H1299 cells incubated with NEM at 37 $^{\circ}\text{C}$ for 2 h, the culture medium was replaced by fresh medium containing biosensor **7** (30 μM) and incubated for another 2 h, and then the hyper-CEST spectrum was obtained. All spectra were acquired at room temperature. All data were fit with Lorentzian line.

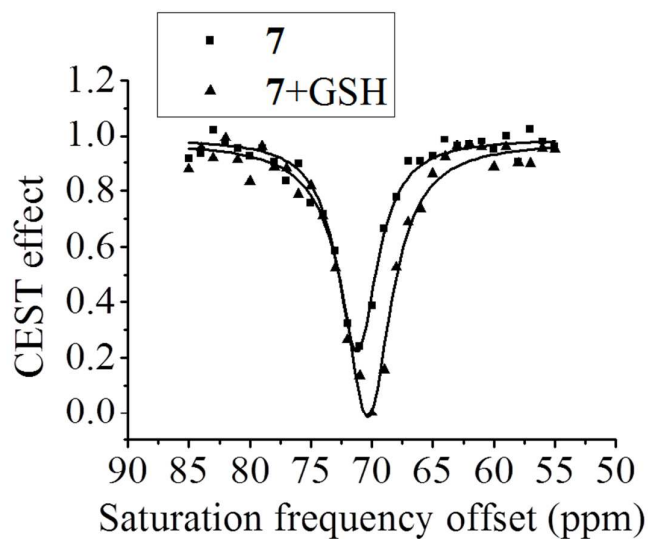


Figure S12. Hyper-CEST spectra of biosensor **7** ($5 \mu\text{M}$) reacted with GSH before and after. (\blacktriangle) After the biosensor **7** reacted with GSH at 37°C for 2 h. (\blacksquare) Before the biosensor **7** reacted with GSH. All spectra were acquired at room temperature in PBS buffer ($\text{pH}=7.4$, 20 mM), containing 50% DMSO (v/v). All data were fit with Lorentzian line.

Table S2. The thermodynamics data of the biosensor **7** reacted with biothiols before and after.

Sample	$f_B (10^{-4})$	$k_{BA} (s^{-1})$
Biosensor 7	8.5 ± 2.9	133.0 ± 75.4
Biosensor 7 +GSH	19.6 ± 5.0	116.8 ± 41.2

9. $^1\text{H-NMR}$, $^{13}\text{C-NMR}$ and ESI-HRMS Spectra

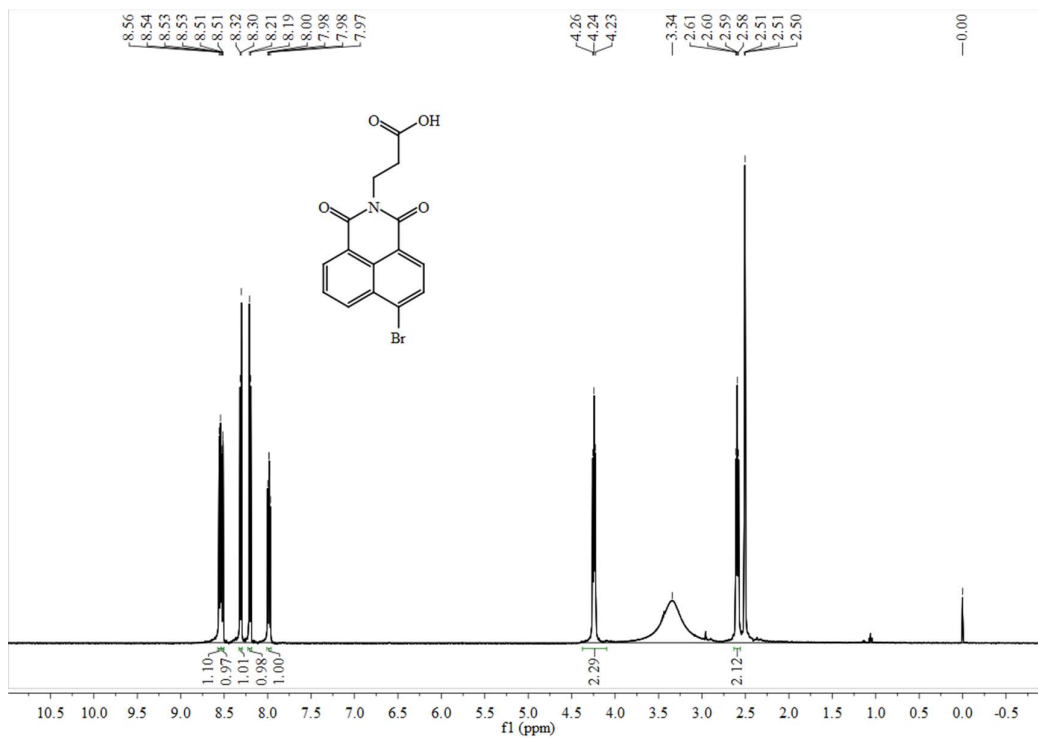


Figure S13. ¹H NMR spectra of **1** record in DMSO-d₆.

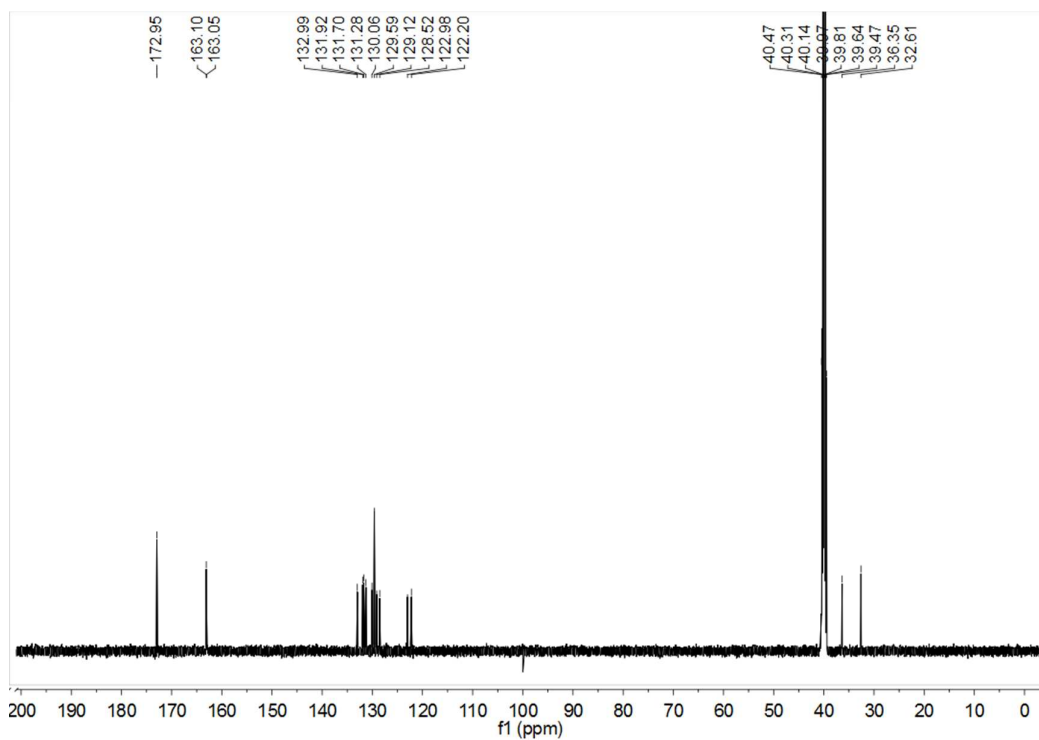


Figure S14. ¹³C NMR spectra of **1** record in DMSO-d₆.

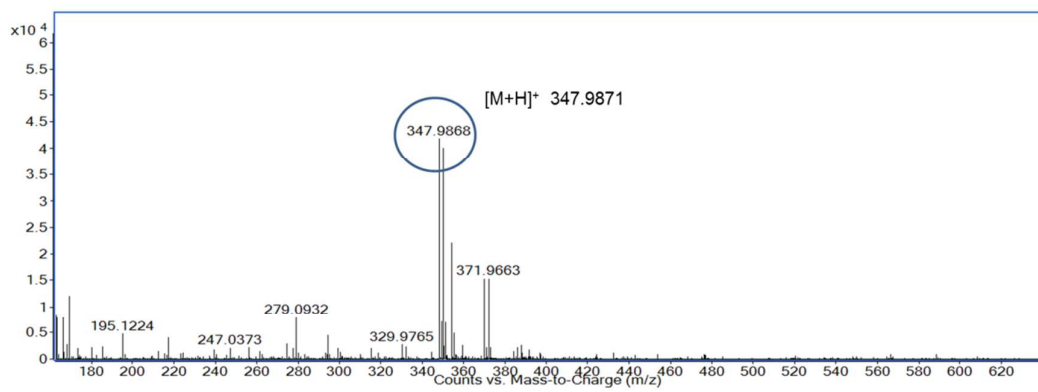


Figure S15. ESI-HRMS spectra of **1**.

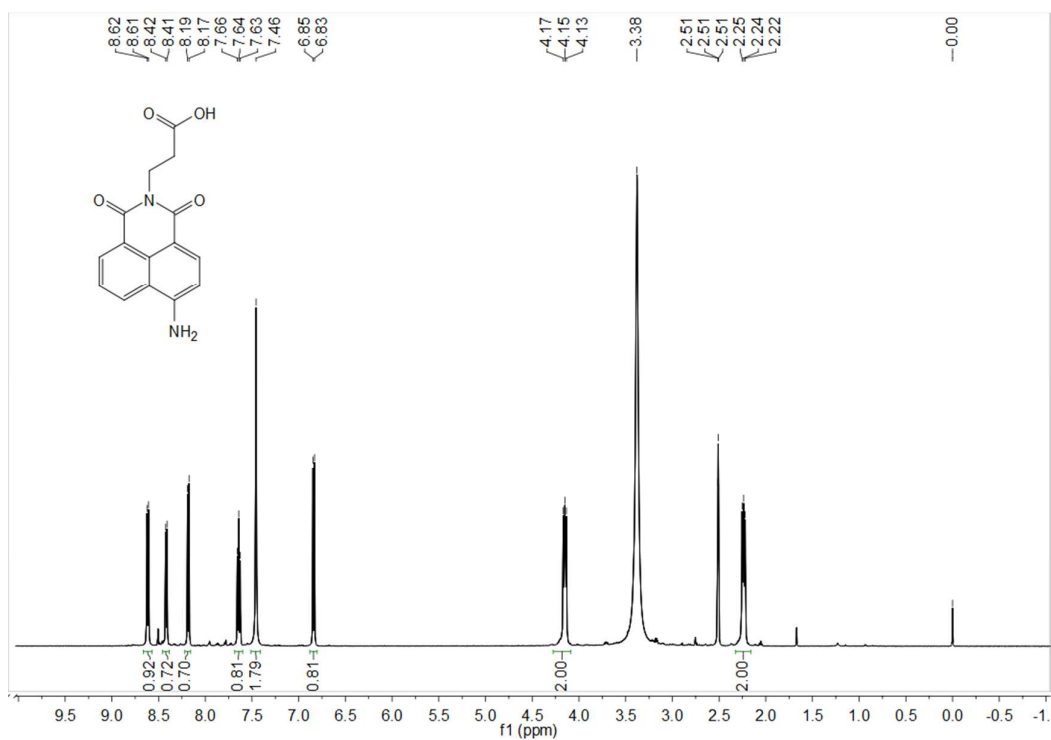


Figure S16. ^1H NMR spectra of **2** recorded in DMSO- d_6 .

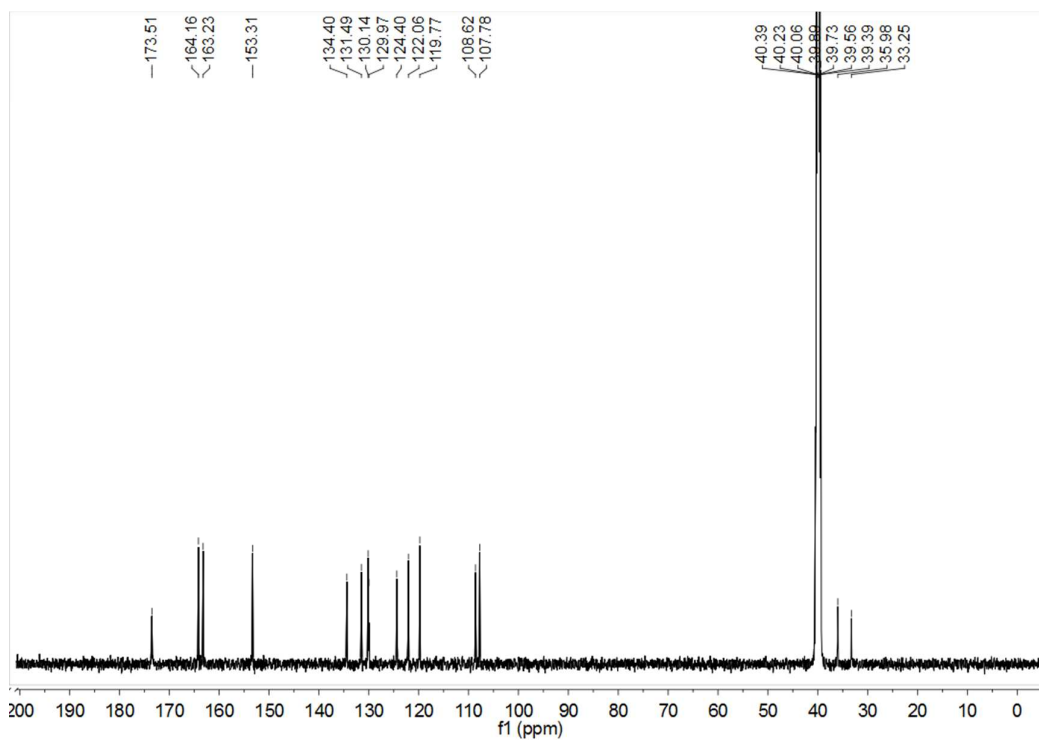


Figure S17. ^{13}C NMR spectra of **2** recorded in DMSO- d_6 .

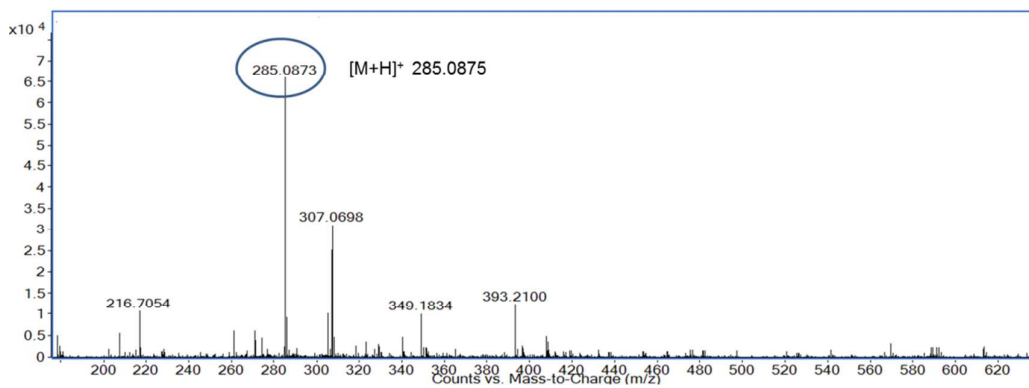


Figure S18. ESI-HRMS spectra of **2**.

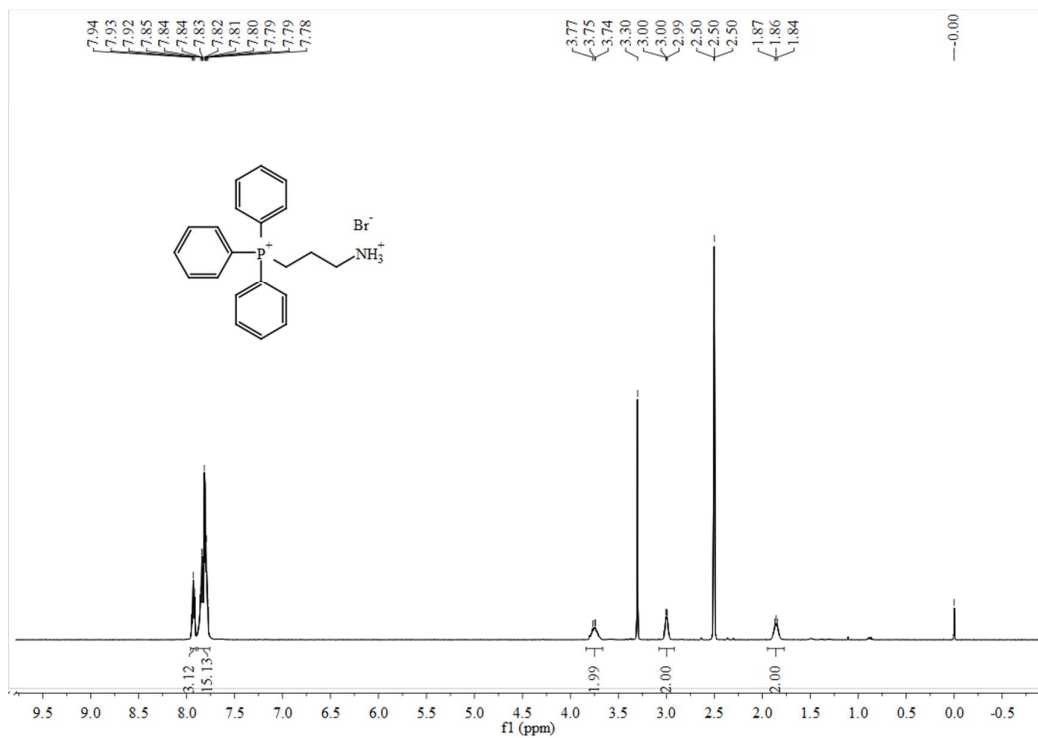


Figure S19. ^1H NMR spectra of **3** recorded in DMSO-d₆.

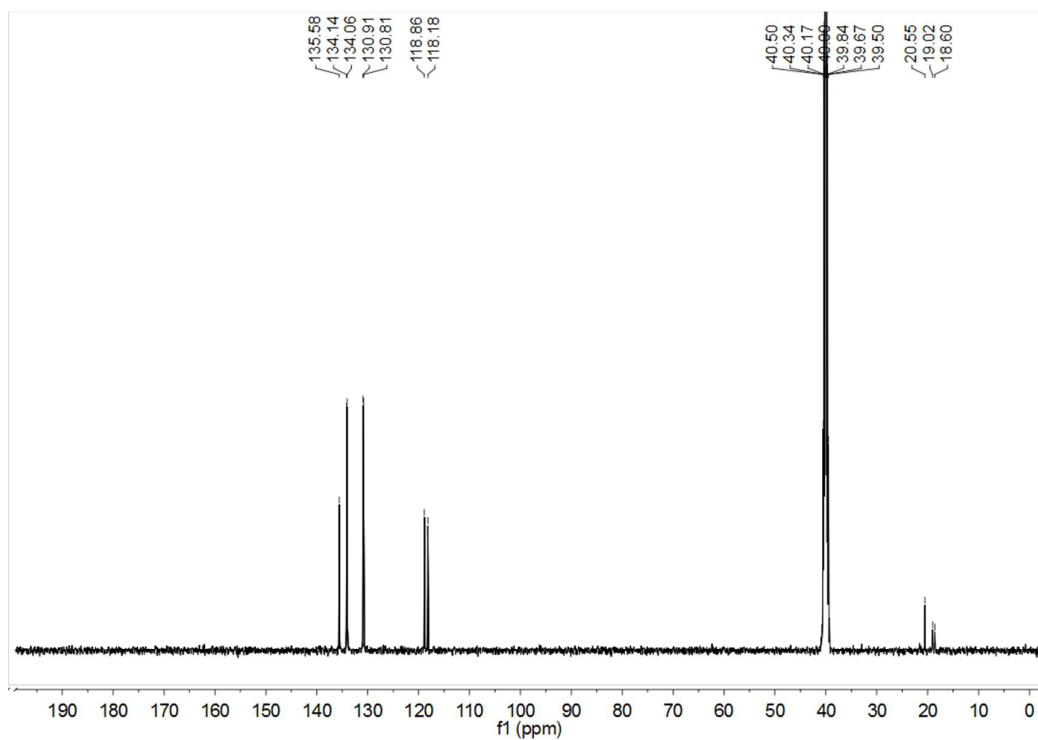


Figure S20. ^{13}C NMR spectra of **3** recorded in DMSO-d₆.

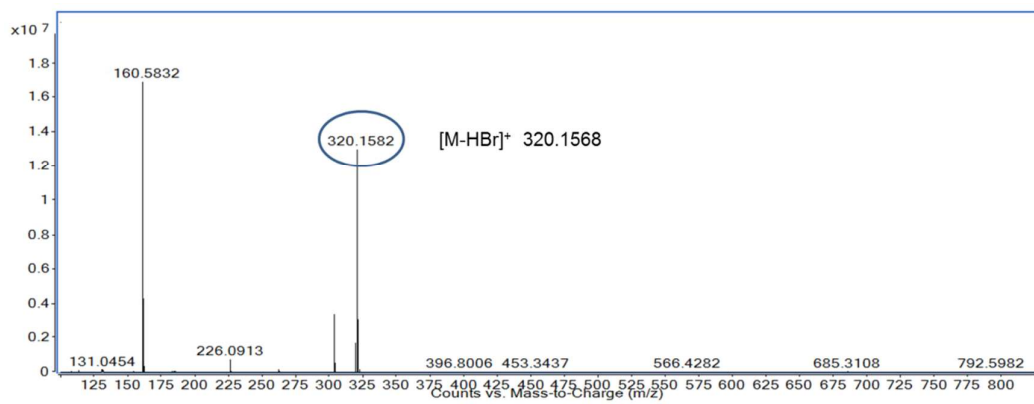


Figure S21. ESI-HRMS spectra of **3**.

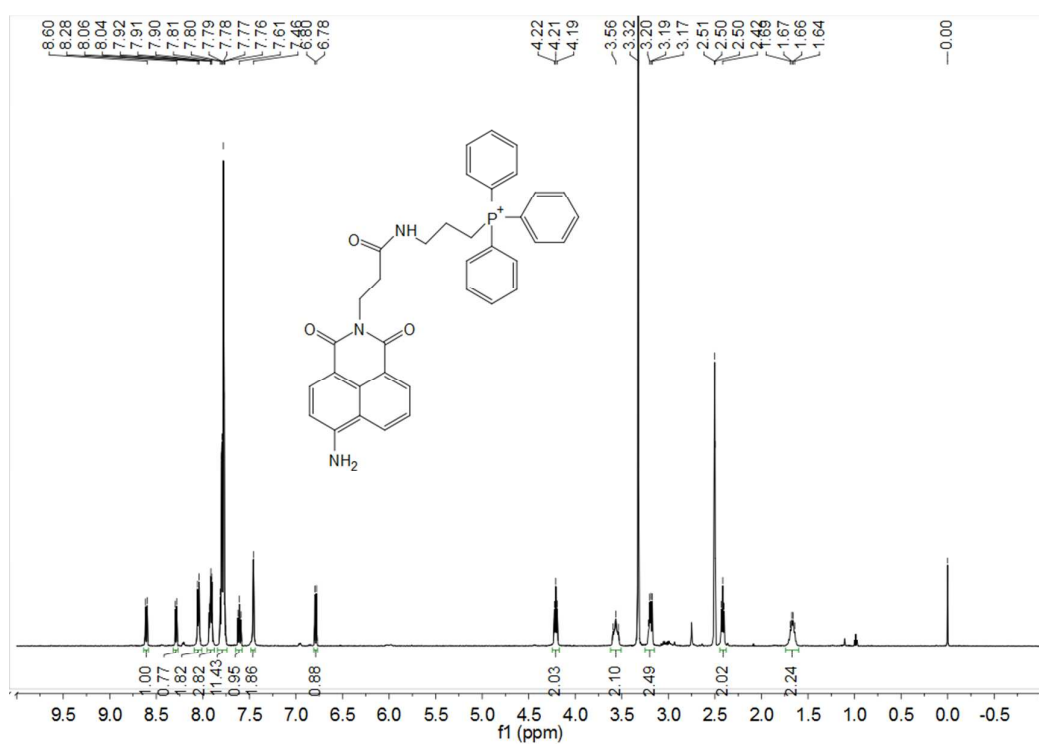


Figure S22. ^1H NMR spectra of **4** recorded in DMSO-d_6 .

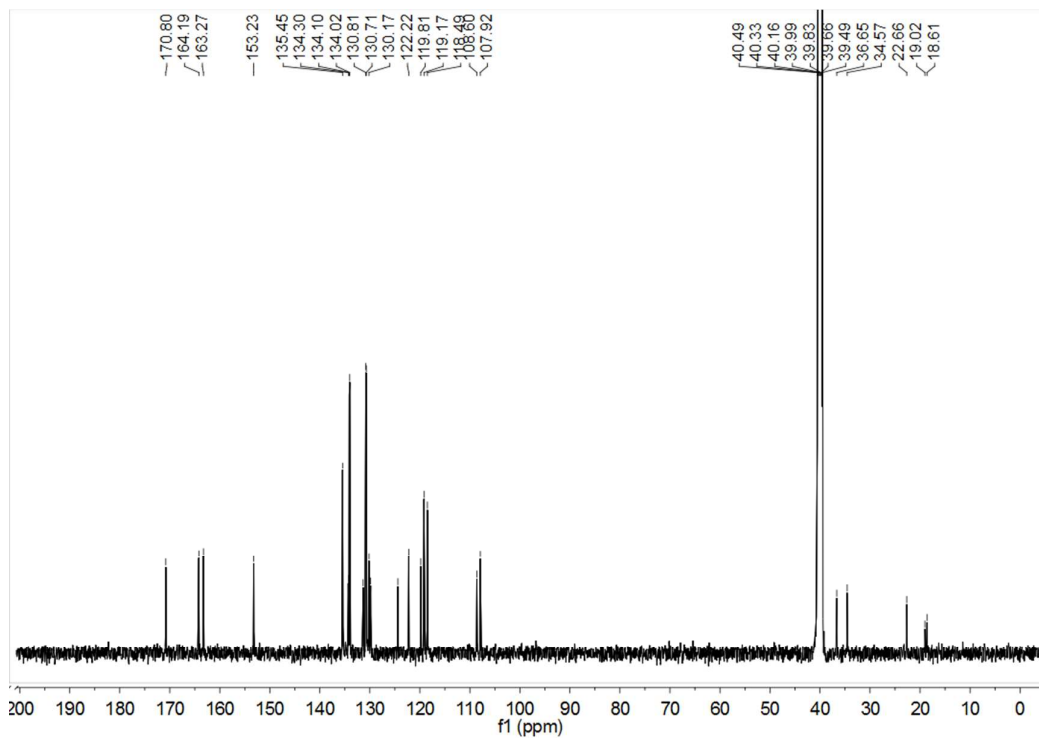


Figure S23. ^{13}C NMR spectra of **4** recorded in DMSO- d_6 .

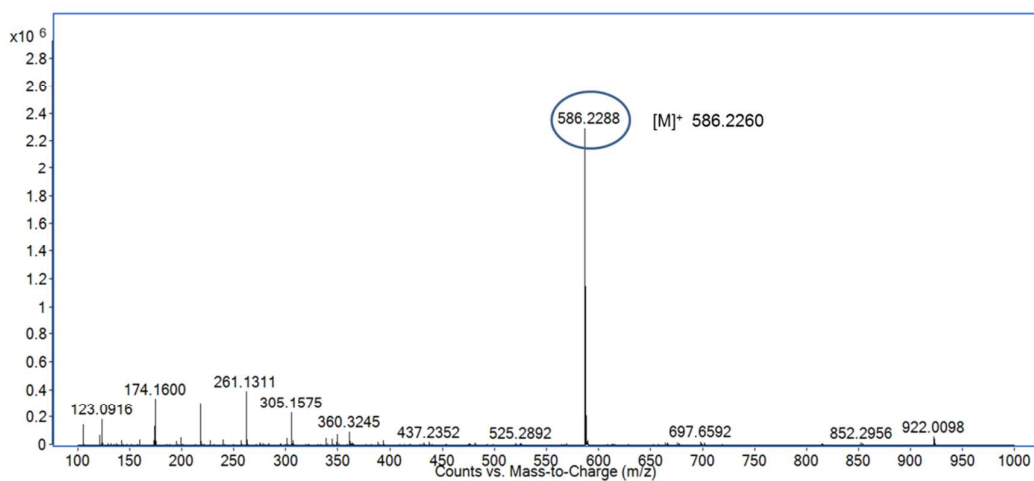


Figure S24. ESI-HRMS spectra of **4**.

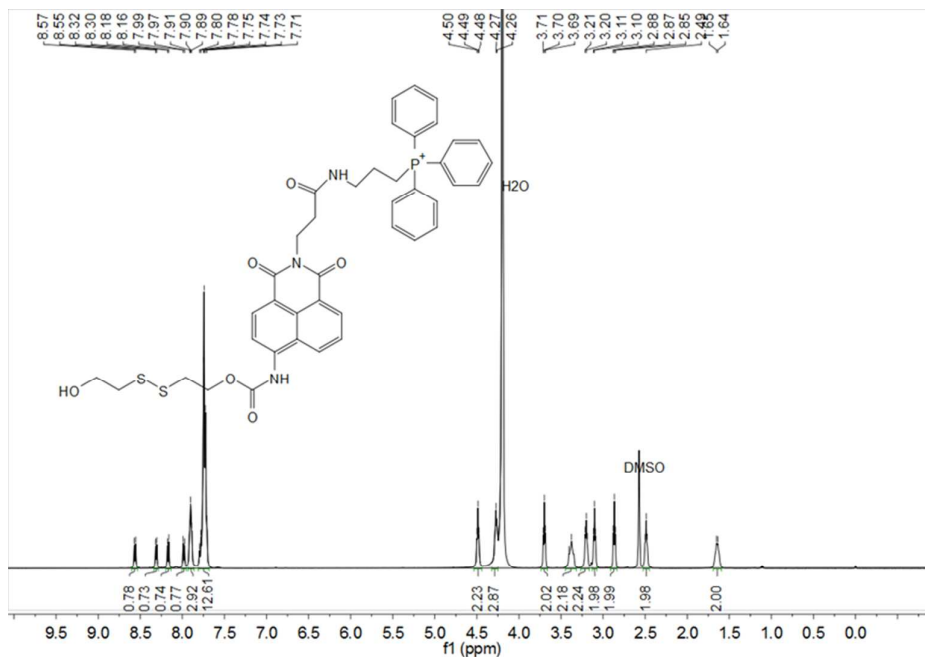


Figure S25. ¹H NMR spectra of **5** recorded in DMSO-d₆.

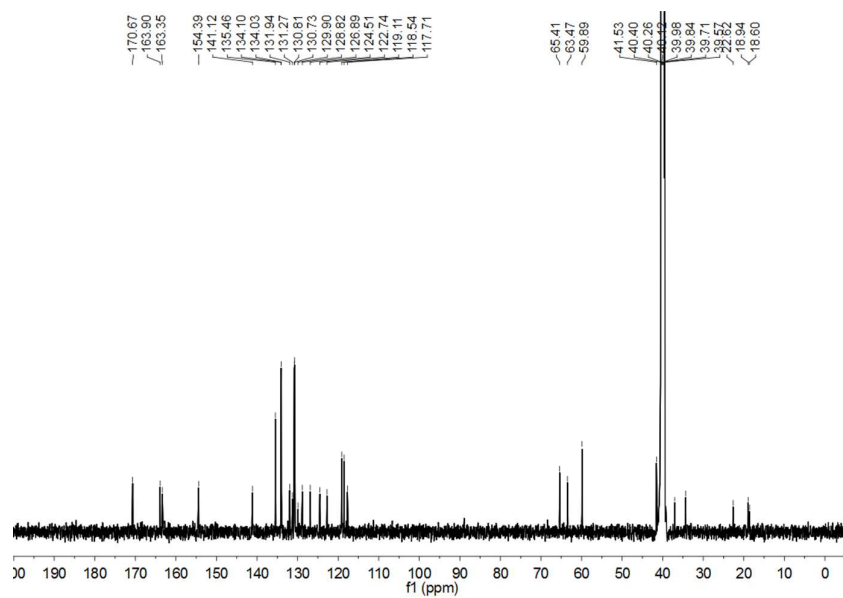


Figure S26. ¹³C NMR spectra of **5** recorded in DMSO-d₆.

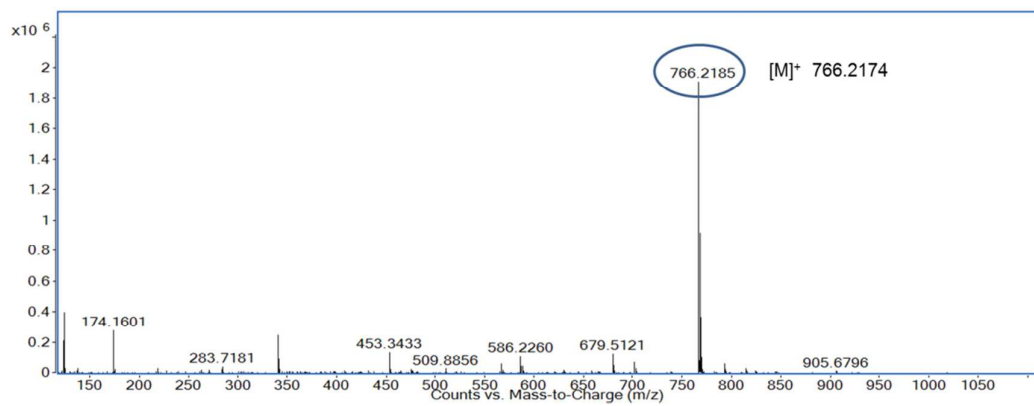


Figure S27. ESI-HRMS spectra of 5.

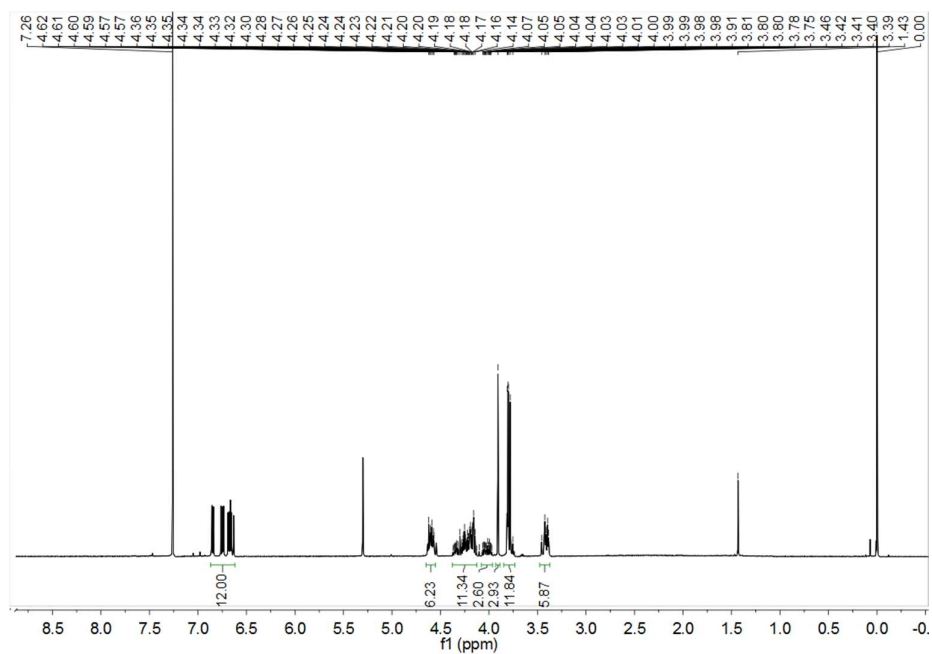


Fig S28. ^1H NMR spectra of 6 recorded in CDCl_3 .

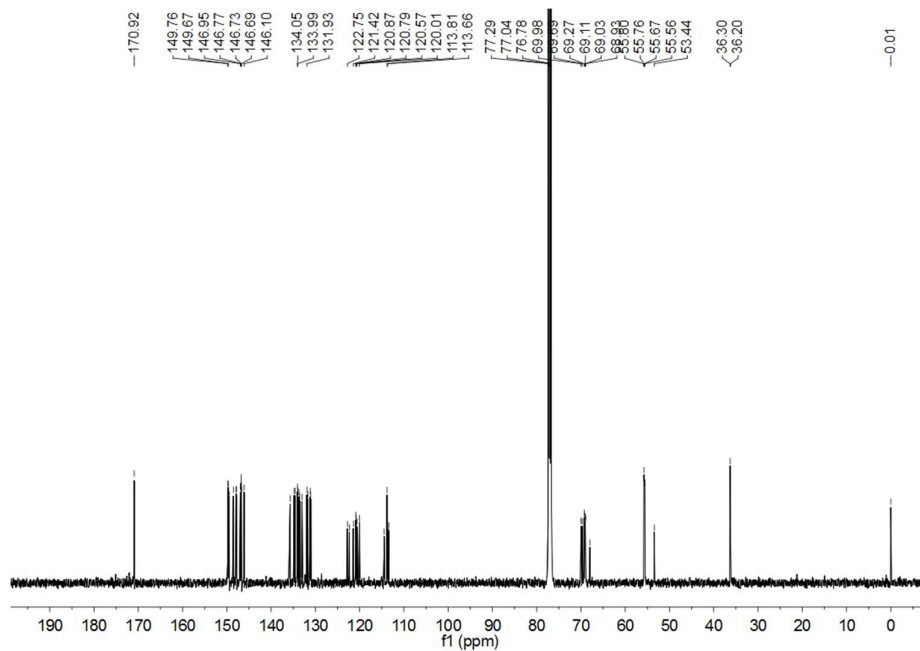


Fig S29. ^{13}C NMR spectra of **6** recorded in CDCl_3 .

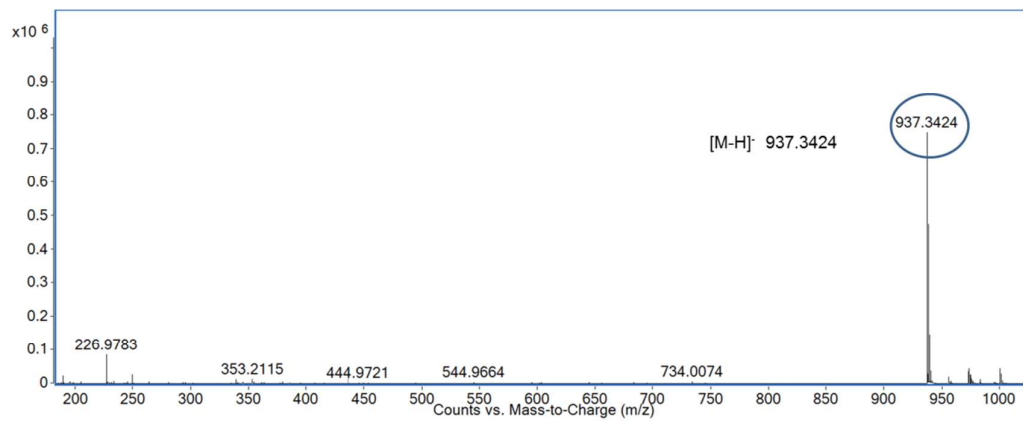


Fig S30. ESI-HRMS spectra of **6**.

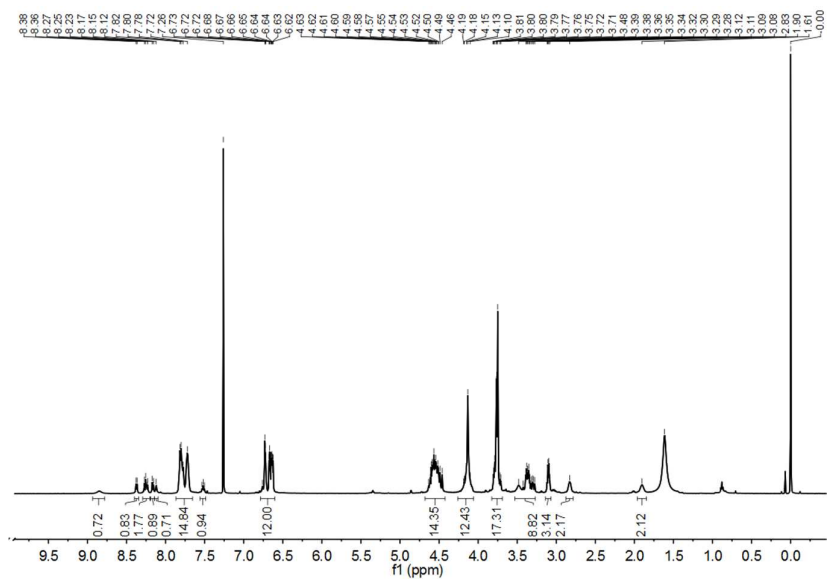


Figure S31. ^1H NMR spectra of **7** recorded in CDCl_3 .

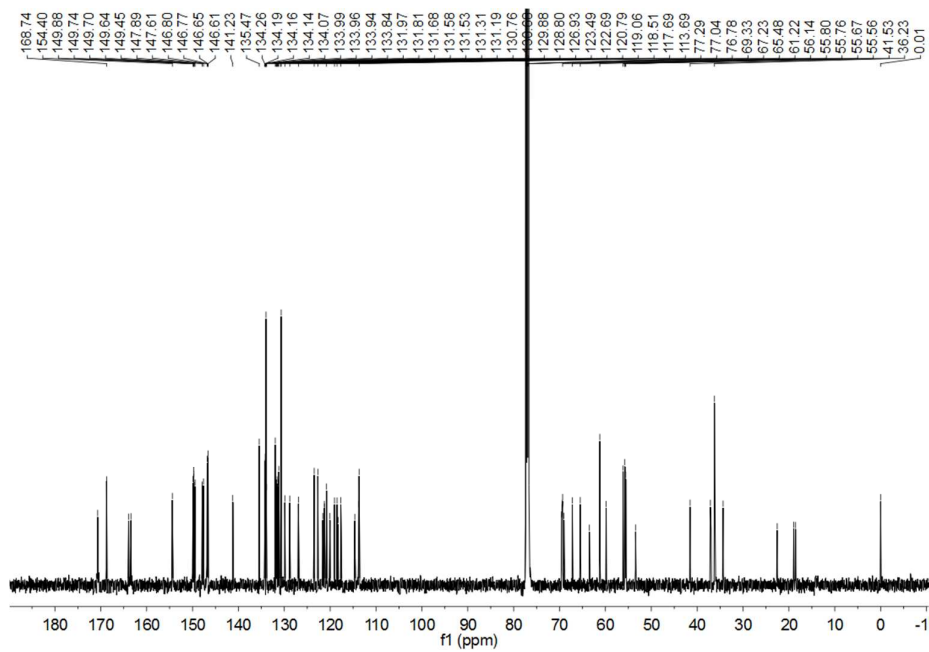


Figure S32. ^{13}C NMR spectra of **7** recorded in CDCl_3 .

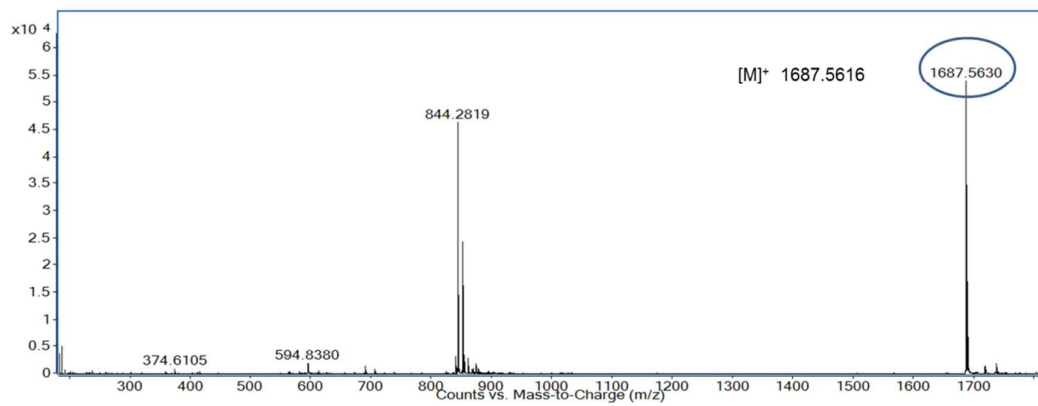


Figure S33. ESI-HRMS spectra of **7**.